*Journal of Electrical Engineering & Technology Vol. 7, No. 5, pp. 765~771, 2012* **765**
http://dx.doi.org/10.5370/JEET.2012.7.5.765

# Breakdown Characteristics of $SF_6$ and Liquefied $SF_6$ at Decreased Temperature

**Eun-Hyeok Choi*, Ki-Chai Kim* and Kwang-Sik Lee†**

**Abstract** – $SF_6$ gas has been used as arc quenching and insulating medium for high and extra high voltage switching devices due to its high dielectric strength, its excellent arc-quenching capabilities, its high chemical stability and non toxicity. Despite of its significant contributions, the gas was classified as one of the greenhouse gas in the Kyoto Protocol. Thus, many researches are conducted to find out the replacement materials and to develop the $SF_6$ gas useless electrical equipment. This paper describes experiments on the temperature change-related breakdown characteristics of $SF_6$ gas ($SF_6$) and $SF_6$ liquid ($LSF_6$) in a model GIS(Gas-Insulated Switchgear) chamber in order to show the possibility of more stable and safe usages of $SF_6$ gas. The breakdown characteristics are classified into three stages, namely the gas stage of $SF_6$ according to Paschen's law, the coexisting stage of $SF_6$ gas with liquid in considerable deviation at lower temperature, and the stage of $LSF_6$ and remaining air. The result shows that the ability of the $LSF_6$ insulation is higher than the high-pressurized $SF_6$. Moreover, it reveals that the breakdown characteristics of $LSF_6$ are produced by bubble-formed $LSF_6$ evaporation and bubbles caused by high electric emission and the corona. In addition, the property of dielectric breakdown of $LSF_6$ is determined by electrode form, electrode arrangement, bubble formation and movement, arc extinguishing capacity of the media, difficulty in corona formation, and the distance between electrodes. The bubble formation and flow separation phenomena were identified for $LSF_6$. It provides fundamental data not only for $SF_6$ gas useless equipment but also for electric insulation design of high-temperature superconductor and cryogenic equipment machinery, which will be developed in future studies.

**Keywords:** $SF_6$ gas, $SF_6$ liquid, Breakdown characteristics

## 1. Introduction

With advances in industry, there have been ever-increasing requirements for high-quality electrical energy, simplification of operation and maintenance, and assurance of reliability and safety in electrical equipment. As a result, the use of electrical devices using the exceptional insulation characteristics of high pressure $SF_6$ gas ($SF_6$) is being established both domestically and internationally [1].

However, the most famous insulation material, $SF_6$ gas crucial problems on two parts. Firstly, it has been classified as a greenhouse gas and its usages are globally limited. Thus there are many researches in order to find out its replacement materials. One of them, dry-air and $N_2/O_2$ mixture gas which have less environmental impact than $SF_6$ are considered to be applied into power equipment. However, knowing that their dielectric strengths are less than 1/3 of $SF_6$ gas, the power equipment which uses these replacement materials has some problems on its safety and insulation level. Secondly, the $SF_6$ gas which is equipped in intense cold regions causes undesirable breakdown accidents. So as these are caused by the process of liquefaction of the gas, it is needed to reveal phenomenon of breakdown in this process [2].

This paper presents the dielectric characteristics of $LSF_6$ in order to show the possibility of the $LSF_6$ usage in electric insulation devices comparing to $SF_6$ gas. At the same time it demonstrates and explains the phenomena of the breakdown in the process of the liquefaction of $SF_6$ gas. To this end, the insulation characteristics of $SF_6$ liquid ($LSF_6$) in a model GIS (Gas Insulated Switchgear) chamber were evaluated on the different forms/arrangements of electrodes into the dielectric materials. This research could also provide the base data for the design of insulation for a high-temperature superconductor and cryogenic equipment.

This paper is organized as follows: Section 2 describes the experimental procedure and the method. In section 3, experimental results are detailed and discussed. Section 4 presents conclusion.

## 2. Experimental Procedue & Method

The exterior of the model GIS chamber designed and produced to research the insulation characteristics of $SF_6$ is shown in Photo 1. The highest voltage allowed is AC 300

† Corresponding author: Graduate School of Electrical Engineering, Yeungam University, Korea. (kslee@yu.ac.kr)
* Graduate School of Electrical Engineering, Yeungam University, Korea. (choieunhyuck@ynu.ac.kr)
Received: January 21, 2011; Accepted: June 8, 2012

kV. DY-106-Korea (AC 300 kV / 120 mA) was used as the electricity source. In order to observe the inner temperature of the model GIS chamber, a temperature sensor (UNICON, -90 ~+90 ℃) was installed 80 mm away from the vertical central axis, parallel to the electrode at the center of the experimental chamber's interior. A pressure gauge (WISE, 0~1520 kPa) was installed to measure the chamber's inner pressure. The interior pressure of the chamber can be maintained up to $5\times10^{-4}$ Torr using a vacuum pump (SINKU KIKO Co. Ltd, GUD-050A, pumping speed 60 ℓ/min) and a heat-insulating vacuum layer was constructed between the interior and the exterior of the chamber. A window (diameter 110 mm, thickness 20 mm) was installed to allow the observation of the temperature sensor and the electrode installed inside the model GIS chamber. The material for this window was transparent acrylic and was installed by fashioning a cylindrical shape.

The main specification of the experimental chamber is such that the pressurization of 1013 kPa to be on the safe side for pressure variation (203~810 kPa) and maintaining the secrecy within the model GIS chamber is possible for maintaining pressure. In addition, the insulation is designed so that it can allow up to 300 kV for testing the internal insulation force of the $SF_6$, which has high insulation characteristics, and with which the temperature variation of -90~+90℃ or temperature maintenance is possible.

(a) AC high voltage source (b) The model GIS chamber

**Photo. 1.** AC high voltage source and the model GIS chamber

The used electrodes are a needle (diameter 5 mm, angle of needle point: 20°) and a plane electrodes (diameter 59 mm). Three arrangements of electrodes are used: N-P which means the upper part electrode is a needle and the lower part is a plane, P-N which is inversed to N-P arrangement, and P-P using two plane electrode for both the upper and the lower part.

Following is the experimental method for the breakdown characteristics of $SF_6$ in temperature decline. The phase transition characteristics and Breakdown Voltage ($V_B$) were evaluated when the temperature was ranged in -40 ~+30 ℃ which is measured by temperature sensor in each pressure after ventilating the inner chamber to $10^{-4}$ Torr before inserting $SF_6$ with 405, 507, and 607 kPa. The experiment with $LSF_6$ shows that after ventilating the model GIS chamber up to $10^{-4}$ Torr and maintaining $SF_6$ at 304 kPa, $SF_6$ is liquefied until the electrodes are sunk into $LSF_6$. The resulting Breakdown Voltage ($V_B$) characteristics were evaluated. For the voltage of the breakdown characteristics, the average value of ten measurements was used. It is measured after about ten times discharges. The voltage was set to the rising speed of 1 kV/s during the $V_B$ measurement.

The next section shows the experimental results following above experimental procedure and the method.

## 3. Experimental Results & Discussion

### 3.1 Temperature dependence with the maintenance of a fixed amount of gas, breakdown characteristics and phase transition characteristics

Fig. 1 shows the $V_B$ in specific pressure of $SF_6$ in N-P electrodes versus temperature. A fixed amount of $SF_6$ is maintained at 405, 507 and 607 kPa at 30 ℃. The purpose of this condition is to identify the inner status of $SF_6$ and its insulation characteristics according to changes in the power equipments' temperature, using $SF_6$ in severely cold areas.

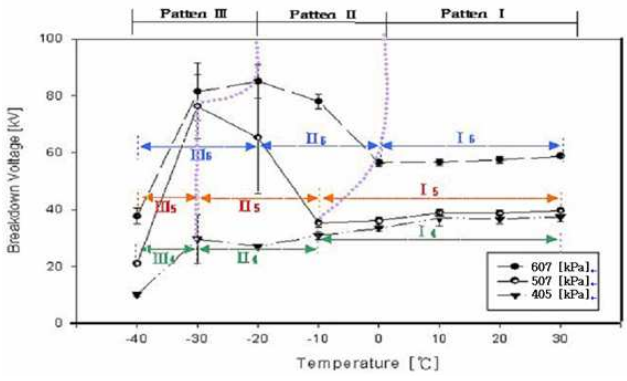


**Fig. 1.** The characteristic of breakdown versus the temperature with constant gas volume

In Fig. 1, Pattern I is a phase where pressure decreases according to temperature at a gaseous state toward each pressure. At this time, the pressure gradually decreases as the temperature drops and there is a section where the $V_B$ also drops. In other words, this is a field where Paschen's

law is applied.

Pattern II is a process where the $SF_6$ is gradually being liquefied in a chamber. The liquefaction of $SF_6$ is started from the upper part of the chamber where the dry-ice is attached. The liquefied $SF_6$ surrounds the needle electrode area and inner wall of the chamber and leads the increase of breakdown voltage. The phenomenon of voltage increase at this phase is indicated in Fig. 2. While $LSF_6$ covers the needle electrode (Fig. 2(b)), it is obvious that there is a great deal of deviation in the $V_B$ value due to the enclosing $LSF_6$ of the electrode.. As increasing the quantity of $LSF_6$ enclosing the needle electrode (Fig. 2(c)), its drop becomes falling down (Fig. 2(d)). After that $LSF_6$ is dropped onto the lower part and the plane electrode (Fig. 2(e)), the value of $V_B$ decreases. This is the step where liquefaction is in progress and the insulation media between N-P displays the insulation characteristics of a field where $SF_6$ and $LSF_6$ coexist. Finally, $LSF_6$ is covered on the plane electrode (Fig. 2(f)).

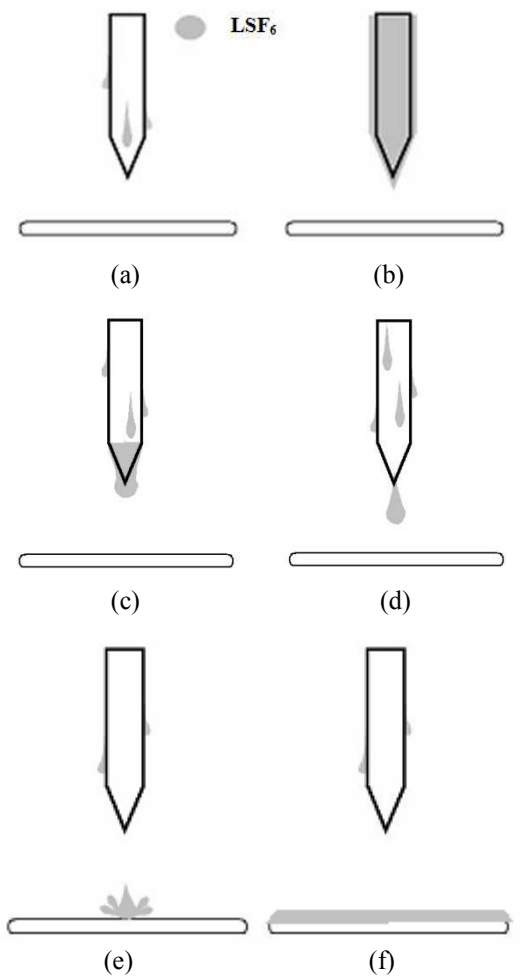


**Fig. 2.** The $LSF_6$ climbs down along to the electrodes: (a) Started liquefaction; (b) $LSF_6$ surrounds the needle electrode; (c) Set up an $LSF_6$-drop; (d) An $LSF_6$-drop; (e) Right after the $LSF_6$, which was surrounding the needle electrode area, was dropped; (f) Film $LSF_6$ at the plane

The pattern II is is also figured in Photo 2. $SF_6$ gas starts being liquefied because of temperature declining. In this temperature range, there is the actual point of liquefaction of the gas. Photo 2(a) shows the behaviors of $LSF_6$ drops. The upside of chamber is attached to a refrigerant, namely, dry ice. Since the liquefaction has progressed from the upside, the drops of $LSF_6$ are formed at this place. Then the drops flow both onto the electrodes and the inner wall of the chamber. Photo 2(b) shows the plane electrode which is covered by $LSF_6$. Moreover, liquefaction occurs at a lower temperature if the gas pressure is low.


1: The $LSF_6$, at the upper chamber area, was dropped.
2: The $LSF_6$ flows on inner wall of chamber
3: The $LSF_6$ flows on needle

(a) A formation part of the typical $LSF_6$

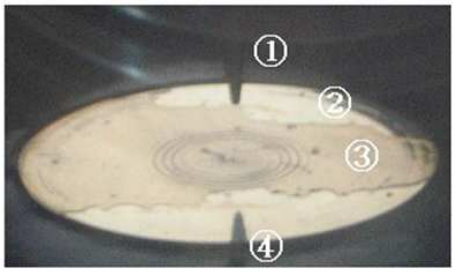


1: Needle 2: Plane
3: Formed film $LSF_6$ at Plane
4: Reflected needle form

(b) $LSF_6$ on the plane

**Photo 2.** A process where the $SF_6$ is being liquefacted in the chamber

Moreover, liquefaction occurs at lower temperatures if the gas pressure is low according to Boyle-Charles's Law and the phase balance. As shown in Fig. 2, the $SF_6$ exists as gas from 0~20℃, -20~-10℃, and -30~-20℃ at 607, 507 and 405 kPa, respectively. When the temperature of electrode gets lower than 0℃, the liquefaction begins at the highest area of the chamber, which has the lowest temperature in the chamber. The most active liquefaction

occurred when the electrode's temperature was at -20℃. Moreover, the liquefaction began at -30~-20℃ at 405 kPa. Since the chamber's temperature sensor was installed 150mm from the floor, which is 80 mm away from the horizontal center parallel to the electrode, the actual liquefaction point would occur at higher temperature than measured temperature.

In pattern III, most of the $SF_6$ inside the chamber is liquefied. $LSF_6$ is collected at the lower part of the model GIS chamber. Consequently, there exists the extremely low pressure of $GSF_6$ near the upper part of the chamber. The upper area surrounding the electrode gets filled with mixture of non-liquefied $SF_6$ gas and the remaining air that could not be ventilated. This is the step where the $V_B$ becomes considerably low. This is the reason of the malfunction of GIS using $SF_6$ in an intense cold region.

### 3.2 $V_B$ characteristics of $LSF_6$

The model GIS chamber used in this research contains a vacuum layer between the inner and outer chambers for heat insulation. Bubbles are created under a certain pressure of $LSF_6$, and a further increase in the bubbles is followed by the creation of a corona discharge. The flow of the increasing bubbles becomes separated from the boundary by electrodes that are arranged vertically so that a recycling form is created in this field. This phenomenon is called Separation and it is created more easily on the plane.

From the above results which show the liquefied $LSF_6$ has a strong dielectric characteristic, the different types of electrodes are used for detailed evaluations of the characteristics of $LSF_6$. The GIS chamber is fulfilled by $LSF_6$ and the electrodes are also immersed in $LSF_6$. Fig. 3(a) shows the breakdown characteristics of $LSF_6$ under the different distances of electrodes according to the types of arrangement of electrodes. The arrangements of electrodes are follows: N-P and S-P, P-P and P-N. As the distance (d) is far, $V_B$ increases for all cases.

When the gap distance is 1mm, $V_B$ for all the types of arrangement are similar, since the short distance leads the uniform electric fields. When d is over than 1 mm, increase of $V_B$ under S-P and P-P arrangements are higher than under P-N and N-P forms. It is also explained by their electric fields. S-P and P-P arrangements keep uniform electric fields in a distance from 1mm to 4mm. In addition, there exists the strong bubble effect under P-P. It is why the $V_B$ under P-P arrangement is lower than $V_B$ under S-P at d=4mm.

Then, P-N and N-P arrangements cause non-uniform fields. Because of this unbalance of the field, the $V_B$ becomes lower. However, the $V_B$ under P-N is higher than under N-P. So as the plane electrode is negative polarity under P-N, it is more difficult to engender the corona discharge because of the feature of electrode. Although it is possible that the bubble is more under P-N arrangement, the bubble of $LSF_6$ still has good arc-quenching capabilities. Thus, the negative plane electrode would keep being difficult to generate the corona discharge and making $V_B$ higher.

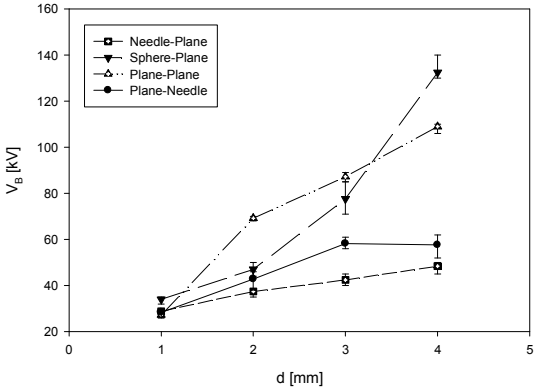


(a) $LSF_6$

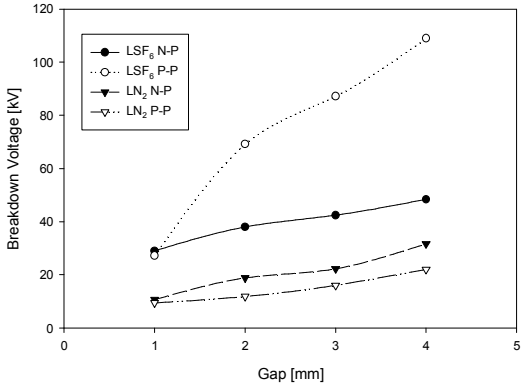


(b) $LSF_6$ and $LN_2$

**Fig. 3.** The Breakdown voltage characteristics in $LSF_6$ and $LN_2$

Fig. 3(b) shows the Gap (d)-$V_B$ characteristics under N-P and P-P arrangements in $LSF_6$ and $LN_2$ when the electrodes are connected to AC power. The $V_B$ of $LN_2$ under N-P and P-P electrodes are surely lower than the $SF_6$'s. However, on the contrary to the cases for $SF_6$, the $V_B$, $LN_2$ under P-P electrodes is lower than under N-P electrodes, since there is no positive bubble effects in this medium compared to $LSF_6$. It shows that the dielectric strength of $LSF_6$ is high and this characteristic is caused by the electric field and the bubbles. However, while d increases comparatively, the $V_B$ under the N-P, and P-P electrodes increase, especially in the P-P.

### 3.3 The $LSF_6$ bubble movements

There is a phenomenon that $V_B$ under P-P is higher than the N-P.The authors call this the "Positive Bubble Effect". Under the consideration of bubble generation and the exercise characteristics, the Positive Bubble Effect can be

defined as follows:

(1) In the beginning, when the air pressure for the $LSF_6$ is 406 kPa, the temperature of liquefaction is approximately -20 ~ -30 ℃.

(2) $LSF_6$ has natural bubbles and bubbles caused by corona. The $SF_6$ bubbles in the $LSF_6$ ($BSF_6$) have good arc cancellation abilities. Therefore, the corona and arc in the bubbles found in $LSF_6$ degrade very quickly.

In the results, in the case of the $LSF_6$, the possibility of bubbles existing inside the chamber degrade. In the $LSF_6$, the breakdown caused by the electric field is more important than the breakdown caused by the bubble effect. The P-P electrode, which is the sub balanced electrode shape, has a higher $V_B$ than the N-P's, which has an extremely unbalanced electrodes.

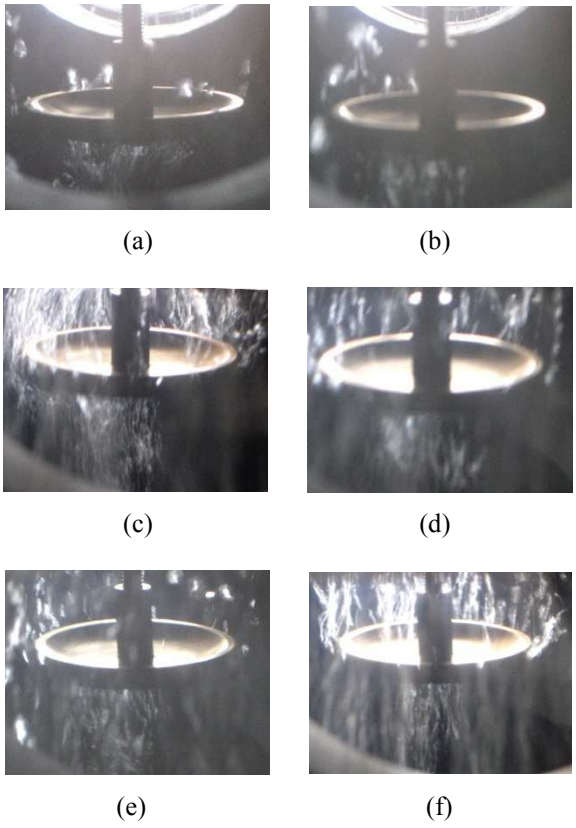


**Photo 3.** The occurrence and separation of the bubbles (P-N, d=6 mm, V=20 kV): (a) Before voltage connection; (b) Just after voltage connection; (c) 60 s after voltage connection; (d) 120 s after voltage connection; (e) Just after voltage disconnection; (f) 30 s after voltage disconnection

Photo 3 shows the occurrence and separation of the $BSF_6$. The flow of a liquid is usually separated from its boundary and a recirculation form is produced in its area.

Photo 3(a) is the photograph before voltage connection. The natural $BSF_6$ elevating from the lower part moves upwards along the surface of the needle electrode. Photo 3(b) shows the bubble separation phenomenon just after voltage connection. In this case, the bubbles are formed in a fan shape, as shown in the photo, due to the heat of the corona at the needle end. The production of bubbles increases at the side of the needle electrode and the needle end with progress of the corona. As shown in Photo 3(c), in terms of bubbles produced by the corona, the bubbles elevating over the plate electrode gradually increased with lapse of voltage connection time. As illustrated in Photo 3(d), when the maximum quantity of bubbles is reached, the elevating speed of the bubbles also becomes maximal. In general, the speed of flow of a viscous fluid is reduced near the boundary due to viscous resistance compared to the speed of irrotational flow. The speed of bubbles existing at the lower part of the plate electrode becomes near zero (0) and they are shown as static bubbles. Therefore, static bubbles form the $SF_6$ gas layer at the back of the moving direction (the lower part of the plate electrode).

In addition, at the lower part, where separation is produced, the bubbles at the outside of the separation surface move very rapidly and those at the inside move relatively slowly. As described, the high velocity gradient at the separation surface produces an eddy phenomenon and the eddy of bubbles may clearly be identified at the back side of the plate where the bubbles are most actively produced, as shown in Photo 3(d).

It was noted that when the voltage was disconnected, the production of the corona was rapidly reduced and the elevating speed of the bubbles was also significantly reduced, as indicated in Photos 3(e) and 3(f).

### 3.4 $V_B$ characteristics contrast needle-plane with plan-needle

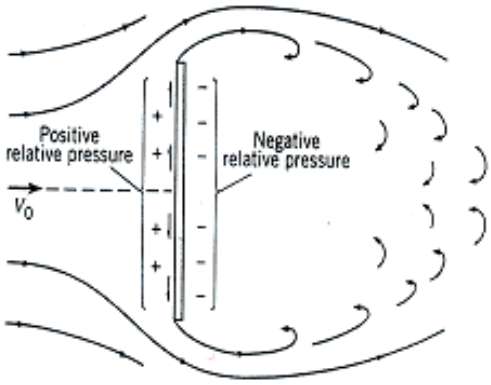


**Fig. 4.** The bubble-flow to pass at plan

Although the experimental imitation GIS chamber used in this research has placed a vacuum layer between inner and outer chamber for heat insulation, the bubbles are created under certain pressure of $LSF_6$ and such bubble gets increased even more followed by creation of corona.

The flow such bubbles becomes separated from the boundary by electrodes that are arranged vertically as they get increased so that a recycling form is created in this field. Such phenomenon is called the 'Separation' and is created more easily on the plane electrode.

If the relative effect of pressure and viscosity force on resistance followed by separation is examined, both pressure and viscosity force act on the plane in case the flat board has been vertically placed. But the viscosity force acts in vertical direction and forms symmetry toward the midpoint of the flat board. Therefore, the viscosity force does not contribute to the dynamic lift or resistance directly. As shown in the Fig. 4, the difference of pressure at upper bubble section and lower bubble section of the plane is created the movement of bubbles. Thus, the pressure of upper section gets relatively increased. Fig. 5 shows the $V_B$ comparison between N-P and P-N.

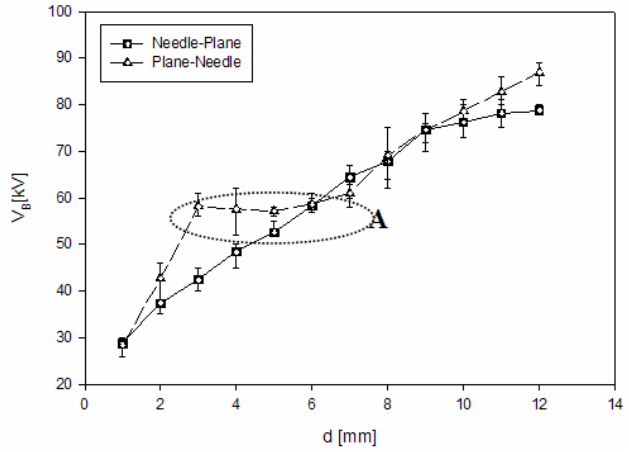


**Fig. 5.** Breakdown characteristics under N-P with P-N.

Fig. 5 shows the $V_B$ comparison between N-P and P-N. For the N-P arrangement, d-$V_B$ rises almost linearly. On the other hand, as the d increases, the section (A) in which $V_B$ gets saturated exists. In the experiment, the bubble moves following the surface of electrode by being separated as bubbles collide vertically to plane electrodes placed in perpendicular direction with the progressing direction of bubbles while the bubbles which exist by touching the electrode surface get to move toward the edge of plane electrode as they get attached to the electrode. In this process, the pressure gets relatively increased at upper stream section due to separation. Therefore, the density of bubbles becomes increased at upper stream section and the speed of movement toward the edge gets relatively faster. Since bubbles created in $LSF_6$ have extremely high arc cancellation abilities to create bubbles from bubble or corona, the creation of arc in such bubbles are cancelled quickly. As consequent, the bubbling condition becomes weak in $LSF_6$.

## 4. Conclusions

This paper described the breakdown characteristics of $SF_6$ liquid ($LSF_6$) based on the phase change of $SF_6$ gas ($SF_6$) under declined temperature. As being progressed the liquefaction of $SF_6$, the breakdown voltage($V_B$) increased, because the $LSF_6$ covered the electrodes of the test chamber. Even though the chamber was not fulfilled by $LSF_6$, the $V_B$ was higher than the one of $SF_6$ at normal temperature. After that most of $SF_6$ liquefied and that $LSF_6$ which was covered the upside electrode kept going on be dropped on the downside electrode, the $V_B$ became decreased. It is due to the low $V_B$ characteristics of remained air and low pressurized $SF_6$ gas. These results show good insulation characteristics of $LSF_6$ comparing to $SF_6$ gas and the possibility of the $LSF_6$ usage in electric insulation devices. Moreover, the comparison study with different types/arrangements of electrodes in $LN_2$ and $LSF_6$ were also achieved. Due to the positive bubble effect of $LSF_6$, the $V_B$ under P-P was higher than the $V_B$ under N-P. This result is contrary to the cases in $LN_2$ which had not the same effect. The positive bubble effect of $LSF_6$ helped degrading the corona discharge in the chamber.

This research provides fundamental data not only for SF6gas useless equipment but also for electric insulation design of high-temperature superconductor and cryogenic equipment machinery, which will be developed in future studies.

### 4.1 The temperature according to the fixed amount of gas-pressure $V_B$ characteristics

(1) At the Pattern I of Fig. 1, the characteristics of $SF_6$ gas follow the Paschen's Law at each pressure.

(2) $SF_6$ gas gradually liquefies from the needle electrode area and the inner walls of the chamber during temperature declining. As the drops of $LSF_6$ climbs down to the needle electrode, the $V_B$ increases considerably. This phenomenon strongly occurs when the $LSF_6$ surrounds the needle electrode area. However, there is a great deal of deviation between the highest and lowest $V_B$; the value being low if $V_B$ is measured right after the $LSF_6$ dropped to the lower section (Pattern II of Fig. 1). It shows the dielectric strength of $LSF_6$ is better than $SF_6$'s.

(3) If the liquefaction is progressed further, the surroundings of the upper electrode becomes being filled with low density of $SF_6$ and the remaining air, and the $V_B$ becomes considerably lower by being in an extremely low pressure state (Pattern III of Fig. 1). This condition causes the malfunction of a GIS using $SF_6$ as its insulation gas.

(4) The boiling point where the gaseous $SF_6$ becomes $LSF_6$ differs according to pressure, but in the experiment, liquefaction occurred when the electrode's temperature was about -10℃. The actual

liquefaction point is the upper chamber, where the the refrigerant dry ice is attached. It can be seen that the liquefaction temperature is lower than the temperature in the upper chamber.

### 4.2 $V_B$ characteristic and $LSF_6$ bubble movements

(1) Dielectric breakdown of $LSF_6$ is determined by electrode form, electrode arrangement, bubble formation and movement, arc extinguishing capacity of the media, difficulty in corona formation, and the distance between electrodes.
(2) The bubble formation and flow separation phenomenon were identified for $LSF_6$.
(3) The dielectric characteristics of $LSF_6$ are determined by the electric fields between electrodes and the bubble movements. It is especially observed that the bubbles are generated by the heat of corona discharge under P-N arrangement and affect to the breakdown voltage.

This research provides fundamental data not only for $SF_6$ gas useless equipment but also for electric insulation design of high-temperature superconductor and cryogenic equipment machinery, which will be developed in future studies.

## Acknowledgements

This research was supported by the Yeungnam University research grants in 2010.

## References

[1] Landry, M. et al. "Dielectric withstand and breaking capacity of $SF_6$ circuit breakers at low temperatures" Power Delivery, IEEE Transactions on, pp. 1029 ~ 1035, July 1988
[2] Gong Guoli et al, "The influence of $SF_6$ and $SF_6/N_2$ dissociating products on the electrical performance of several insulating varnishes", Electrical Insulating Materials, pp. 495 ~ 497, 1995
[3] T.Ueda et al, "Discrimination of Partial Discharge Electromagnetic Signal in $SF_6$ Gas from External Noise Using Phase Gate Control Method", IEEE International Symposium on Electrical Insulation, pp. 117 ~ 120, 1996
[4] Kwang-Sik Lee, "A Study on the discharge characteristics of liquid nitrogen at atmospheric pressure", KIEE Vol 45 No 7, 1996.7.
[5] C.Beyer et al. "Influence Reactive $SF_X$ Gases on Electrode Surfaces after Electrical Discharge under $SF_6$ Atmosphere", IEEE Trans, pp. 234 ~ 240, 2000
[6] Kwang-Sik Lee, "A Study on the Discharge Characteristics of Liquid Nitrogen and Gases at Very Low Temperature", KEPCO, 1993.8.
[7] Kwang-Sik Lee, "The Characteristics of Insulation with Temperature Variations of $SF_6$" KIEE Vol 52C No 8, 2003.8
[8] Kwang-Sik Lee, Eun-Hyeok Choi, "The Positive Effect and the Breakdown Characteristics in $SF_6$ and $LN_2$", KIEE Vol 54C No 8, 2005.8

**Eun-Hyeok Choi** was born in Korea in 1977. He received his B.S. degrees in Electrical Engineering from Kyungil University, Korea, in 2003, He received his M.S. and Ph.D. degrees in Electrical Engineering from Yeungnam University, Korea, in 2005, 2009. Currently, Adjunct professor in Electrical Engineering from Yeungnam University.

**Ki-Chai Kim** received the B.S. degree in electronic engineering from Yeungnam University, Korea, in 1984, and M.S. and Dr. Eng. degrees in electrical engineering from Keio University, Japan, in 1986 and 1989, respectively. He was a senior researcher at Korea Standards Research Institute, Korea until 1993. From 1993 to 1995, he was an Associate Professor at Fukuoka Institute of Technology, Japan. Since 1995 he has been with Yeungnam University, Korea, where he is currently a Professor in Department of Electrical Engineering. He received the Shinohara Memorial Young Scientist Awards from the Institute of Electronics, Information and Communication Engineers (IEICE) of Japan in 1988 and received Paper Presentation Awards in 1994 from The Institute of Electrical Engineers (IEE) of Japan. His research interests are in the areas of EMC and small antennas, reducing electromagnetic penetration of metallic enclosure with aperture, and applications of electromagnetic field and waves.

**Kwang-Sik Lee** was born in Korea in 1948. He received his B.S., M.S. and Ph.D. degrees in Electrical Engineering from Yeungnam University, Korea, in 1971, 1973, and 1987, He was 8 ,9th President of The Korean Institute of Illumination and Electrical Installation Engineers. respectively. Currently, he is now a professor at Yeungnam University.